Nuclear Instruments and Methods in Physics Research A 684 (2012) 82–87

Contents lists available at SciVerse ScienceDirect

Nuclear Instruments and Methods in Physics Research A

journal homepage: www.elsevier.com/locate/nima

Prompt gamma tests of $LaBr_3$:Ce and BGO detectors for detection of hydrogen, carbon and oxygen in bulk samples

A.A. Naqvi [a,*], Fares A. Al-Matouq [a], F.Z. Khiari [a], A.A. Isab [b], Khateeb-ur Rehman [a], M. Raashid [a]

[a] Department of Physics, King Fahd University of Petroleum and Minerals, Dhahran, Saudi Arabia
[b] Department of Chemistry, King Fahd University of Petroleum and Minerals, Dhahran, Saudi Arabia

ARTICLE INFO

Article history:
Received 21 February 2012
Received in revised form
4 May 2012
Accepted 13 May 2012
Available online 22 May 2012

Keywords:
LaBr3:Ce and BGO detectors
Prompt gamma neutron activation analysis
Hydrogen
Carbon and oxygen detection in bulk sample
14 MeV neutron beam
Monte Carlo simulation

ABSTRACT

Prompt gamma ray tests of cylindrical lanthanum halide ($LaBr_3$:Ce) and bismuth germanate (BGO) gamma ray detectors have been carried out for detection of hydrogen, carbon and oxygen concentrations in bulk samples via inelastic scattering of neutrons using a 14 MeV neutron-based prompt gamma neutron activation analysis setup. Regardless of its intrinsic activity, the $LaBr_3$:Ce detector showed superior performance than the BGO detector for the detection of hydrogen, carbon and oxygen concentrations in benzene, water, toluene, propanol, ethanol and methanol bulk samples. The BGO detector has a large concentration of oxygen in its detector material and is consequently less sensitive for oxygen detection in bulk samples. Hence, it is not a suitable choice for oxygen determination in bulk samples.

1. Introduction

Recent developments of radiation hardened lanthanum-halide ($LaBr_3$:Ce and $LaCl_3$:Ce) gamma ray detectors with improved light output, decay time and energy resolution [2,3,6,7,12,14,16,19] have widened the scope of applications for the Prompt gamma-ray neutron activation analysis (PGNAA) technique [5,8,10,11,15,17–20]. Although lanthanum halide detectors have an intrinsic activity due to radioactive decay of a naturally occurring unstable La isotope, they have nonetheless been successfully employed in high count rates studies because this type of detector can handle higher count rates than the conventional NaI and BGO detectors [3,14–16]. However, because of their intrinsic activity, lanthanum-halide detectors may not be suitable in low-level counting experiments [2,8].

$LaBr_3$:Ce gamma ray detectors [6,8,10,12,14,15] and $LaCl_3$:Ce gamma ray detectors [2,3,16,19] have outperformed conventional NaI and BGO detector in terms of light decay time, energy resolution and high count-rate handling capabilities [3,16]. Therefore PGNAA setups employing lanthanum halide detectors are expected to have better performance than those employing NaI and BGO detectors.

King Fahd University of Petroleum and Minerals, Dhahran, Saudi Arabia, has acquired a cylindrical $\emptyset 76 \times 76$ mm^2 height lanthanum halide ($LaBr_3$:Ce) and a $\emptyset 102 \times 102$ mm^2 height bismuth germinate (BGO) gamma ray detector for its for element detection in environmental, concrete corrosion, explosive and contraband detection studies as part of its PGNAA program. These applications require detector response measurements over a broad gamma ray energy spectrum ranging from a few keV to tens of MeV. Previously the response of the $LaBr_3$:Ce detector was tested with low energy prompt gamma-ray for its use in environmental studies [15].

In the present study the response of the $LaBr_3$:Ce detector has been tested for high energy gamma rays using a 14 MeV neutron-based PGNAA setup. Prompt gamma rays with a maximum energy of 6.13 MeV were produced through thermal neutron capture and inelastic scattering of 14 MeV neutrons from propanol, methanol, water, benzene and ethanol bulk samples. Moreover, and for the sake of comparison, the response of a 102×102 mm^2 (height $\times$ diameter) BGO detector was also measured for high energy prompt gamma rays from the above bulk samples. Results of the study are presented in the following sections.

2. Photopeak efficiency measurement of the $LABr_3$:Ce detector

Photopeak efficiency of the $LaBr_3$:Ce detector with 347.6 cm^3 volume was determined from a measurement of its intrinsic

* Corresponding author at: Department of Physics, King Fahd University of Petroleum and Minerals, KFUPM Box 1815, Dhahran 31261, Saudi Arabia. Tel.: +966 3860 4196; fax: +966 3860 2293.
E-mail address: aanaqvi@kfupm.edu.sa (A.A. Naqvi).

0168-9002/$ - see front matter © 2012 Elsevier B.V. All rights reserved.
http://dx.doi.org/10.1016/j.nima.2012.05.044

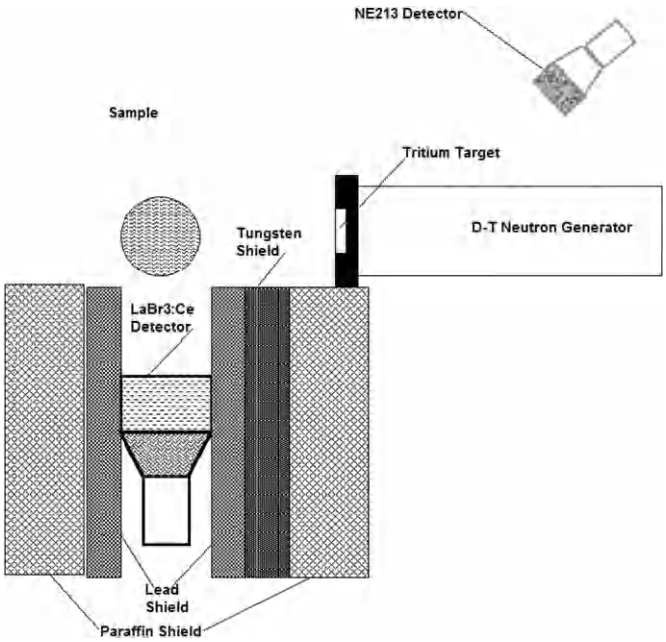

Fig. 1. Schematic of 14 MeV neutron-based setup used for measurement of hydrogen, carbon and oxygen concentration in bulk samples.

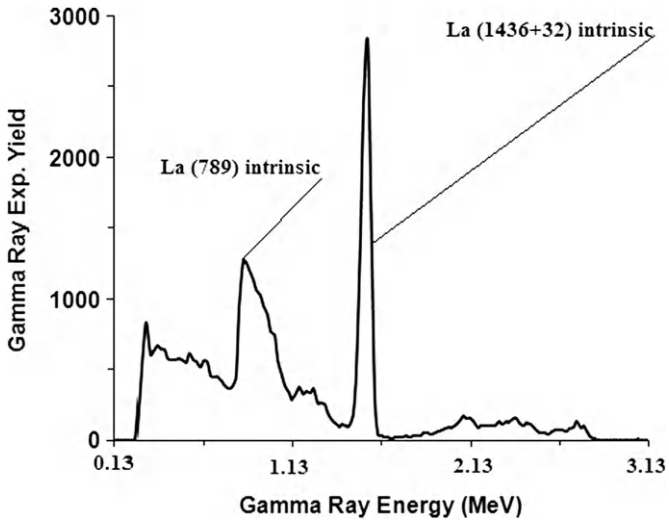

Fig. 2. Intrinsic activity spectrum of the cylindrical 76 × 76 mm^2 (diameter × height) $LaBr_3$:Ce gamma ray detector.

activity. The photopeak efficiency was calculated from the ratio of the measured intrinsic activity count rate and the calculated intrinsic activity of the detector. The intrinsic activity of the $LaBr_3$:Ce gamma ray detector was measured using standard NIM electronics modules described earlier [15]. Fig. 2 shows the pulse height spectrum of the detector recorded over a period of 151 s. It shows the 1468 (1436+32) keV gamma line of the detector's intrinsic activity resulting from the sum of the 1436 keV gamma due to beta decay of ^{138}La isotope and the 32 keV X-ray fluorescence peak due to K shell X-ray fluorescence of Ba produced in the electron capture by La [2,6,8,10]. The intrinsic activity rate was determined from the integrated counts under the 1468 keV peak. It was found to be 63.3 counts/s (0.182 counts/cm^3 s) for the $LaBr_3$:Ce detector. An intrinsic activity of 332 Bq was calculated for the ∅7.6 × 7.6 cm^2 $LaBr_3$:Ce gamma ray detector using the published intrinsic activity data [14]. The calculated photopeak efficiency of the (76 × 76 mm^2) $LaBr_3$:Ce detector was found to be 0.191, which is consistent with the reported values of 0.108 and 0.138 for photopeak efficiency of ∅4.1 × 7.6 cm^2 and ∅5.1 × 7.6 cm^2 smaller cylindrical $LaBr_3$:Ce detectors respectively [14].

3. Prompt gamma rays tests of $LaBr_3$:Ce and BGO detectors

The response of the detector was measured for high energy prompt gamma rays using the 14 MeV neutron-based PGNAA setup shown in Fig. 1. The setup was built around the 0° beam line of the 350 keV ion accelerator [1]. The setup consisted of a ∅9.0 × 14.0 cm^2 cylindrical plastic container filled with the sample material and placed 7.0 cm in front of the water-cooled tritium target, at 0° angle with respect to the 14 MeV neutron beam. The gamma ray detector was placed at a center-to-center distance of 18.9 cm from the sample, at an angle of 90° with respect to the 14 MeV neutron beam. Tungsten blocks were inserted between the tritium target beam line and the gamma ray detector to shield it from direct beam of 14 MeV neutrons. Furthermore, the detector was shielded from the 14 MeV neutron-induced gamma ray background by lead blocks inserted between the detector and the tungsten shield. Finally a paraffin shield was built around the detector enclosing the lead and tungsten blocks, to shield it from room-scattered neutrons. The paraffin shield was prepared by mixing lithium carbonate and paraffin wax in equal weight proportions. Although the paraffin and lead shields were effective in shielding the detector against scattered neutrons and background gamma rays, the gamma ray peaks due to the inelastic scattering of 14 MeV neutrons from lead were quite pronounced in the gamma ray detector pulse height spectrum.

A pulsed beam of 14 MeV neutrons was produced via the T(d,n) reaction using a pulsed deuteron beam with 200 ns width and a frequency of 31 kHz. The typical pulsed beam current of the accelerator was 60 μA dc beam current. As shown in Fig. 1, the fast neutron flux from the tritium target was monitored using a ∅7.6 × 7.6 cm^2 cylindrical NE213 fast neutron detector, placed at a distance of 1.8 m from the target and at a backward angle of 130° with respect to the beam axis on the opposite side of the $LaBr_3$:Ce detector gamma-ray detector. The 14.8 MeV neutron flux was measured to be 10^6n/cm^2/s. The prompt gamma-ray spectrum of the $LaBe_3$:Ce was recorded for a preset time.

3.1. Prompt gamma ray measurements using $LaBr_3$:Ce and BGO detectors

The gamma ray response of the $LaBr_3$:Ce detector was measured for prompt gamma rays produced in the inelastic scattering of 14 MeV neutrons from hydrogen, carbon and oxygen in propanol, methanol, water, benzene and ethanol bulk samples. As shown in Table 1, the hydrogen, carbon and oxygen concentrations of the bulk samples were independently measured using Atomic Absorption Spectrometry in the Department of Chemistry at King Fahd University of Petroleum and Minerals. The samples were prepared by filling the plastic containers with the sample materials and were then irradiated in the 14 MeV neutron based PGNAA setup. Pulse height calibration of $LaBr_3$:Ce was carried out using ^{60}Co source and intrinsic activity peak, while BGO detector pulse height spectrum was calibrated using ^{60}Co source only. The prompt gamma-ray data from the samples were acquired for 25 min using a Multichannel Buffer-based data acquisition system. The neutron flux spectrum was recorded during each run using the NE213 detector, following the procedure described earlier [15], and was used later for neutron flux normalization during data correction. The neutron detector signals were acquired through a single channel analyzer, whose lower level was set at half-Cs pulse height bias electronically set by taking

Table 1
Elemental composition of propanol, methanol, water, benzene, toluene and ethanol samples.

Compounds	Chemical formula	Carbon (wt%)	Oxygen (wt%)	Hydrogen (wt%)
Propanol	C_3H_8O	60.0	26.7	13.3
Methanol	CH_2O	40.0	53.3	6.7
Water	H_2O	–	87.8	11.4
Benzene	C_6H_6	92.3	0.000	7.7
Toluene	C_7H_8	91.3	0.000	8.7
Ethanol	C_2H_6O	52.2	34.8	13.0
Neutron paraffin shielding (Li=9.5 wt%)	$Li_2CO_3+C_{25}H_{52}$ (mixed in equal weight proportions)	50.7	32.4	7.4

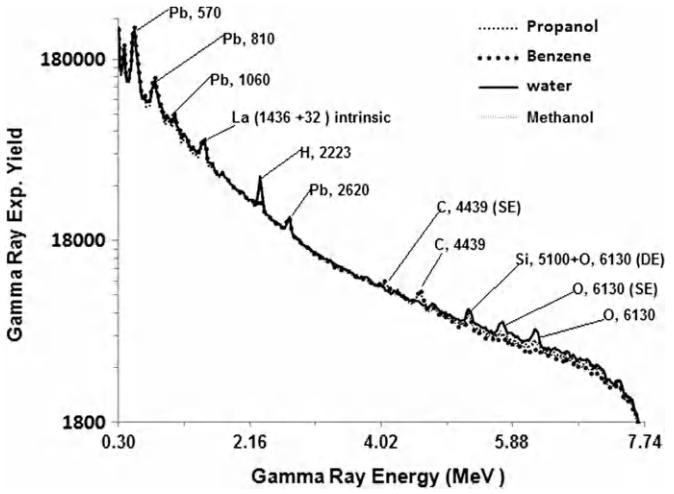

Fig. 3. Full prompt gamma ray spectra of LaBr3:Ce gamma ray detector from activated benzene, propanol, water, methanol and lead shielding.

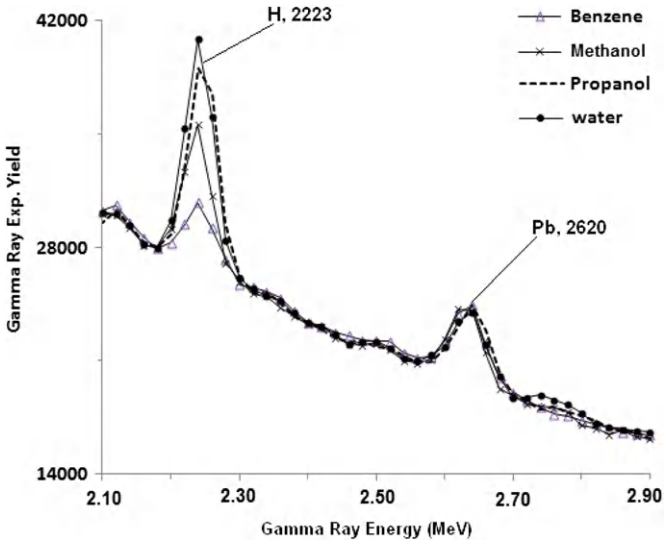

Fig. 4. Enlarged LaBr3:Ce detector prompt gamma ray spectra of benzene, activated propanol, water, methanol and lead shielding plotted over 2.10–2.90 MeV energy range showing hydrogen peak.

Compton edge spectrum of ^{137}Cs gamma ray source with the NE213 detector [15].

Fig. 3 shows prompt gamma-ray pulse height spectra due to the inelastic scattering of 14 MeV neutrons from hydrogen, carbon and oxygen in propanol, methanol, water, benzene and shielding materials over the 0.30–7.74 MeV energy, taken with the $LaBr_3$:Ce detector. The gamma ray energies due to the inelastic scattering of 14 MeV neutrons from lead were previously reported in the literature in Ref. [9]. They were also measured in this study and found at 570, 810, 1060 and 2620 keV. Fig. 4 shows an enlarged portion of the pulse height spectra of Fig. 3 over the 2.10–2.90 MeV energy. It shows the hydrogen peak due to thermal neutron capture by hydrogen in the bulk samples. The hydrogen peak has increasing intensity for the samples with increasing hydrogen listed in Table 1.

Fig. 5 shows the enlarged pulse height spectrum portion of Fig. 3 over the 3.72–6.15 MeV energy range exhibiting the carbon and oxygen peaks due to the inelastic scattering of 14 MeV neutrons from the bulk samples. Fig. 5 shows the single escape (SE) and full energy peaks of 4.439 MeV prompt gamma ray from carbon. For the 6.13 MeV prompt gamma ray of oxygen, the full energy peak along with associated single escape (SE) and double escape (DE) peaks have also been detected and are shown in Fig. 5. The 5.10 MeV gamma rays due to inelastic scattering of 14 MeV neutrons from silicon in walls and floor of the room are interfering with the DE peak of oxygen, thereby increasing the height of the DE peak of oxygen making it higher than the SE peak of oxygen. Also single escape peak of silicon was also detected. The carbon and oxygen peaks intensities have increasing trend with increasing concentration of carbon and oxygen in the samples shown in Table 1. The presence of multiple escape peaks and their interference with other gamma ray peaks of interest in the pulse height spectrum of the $LaBr_3$:Ce detector make the spectrum complex.

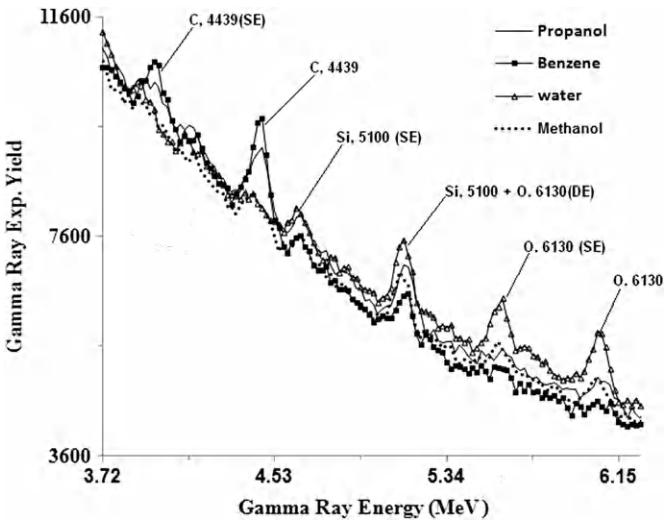

Fig. 5. Enlarged $LaBr_3$:Ce detector prompt gamma ray spectra of benzene, propanol, water and methanol samples plotted over 3.72–6.72 MeV energy range showing carbon and oxygen peaks along with associated escape peaks.

For the sake of comparison, the response of the BGO detector was tested for gamma rays in the same energy range as those used with the $LaBr_3$:Ce detector in the inelastic scattering of 14 MeV neutrons from toluene, propanol, methanol, water, benzene and ethanol bulk samples. Fig. 6 shows the gamma ray

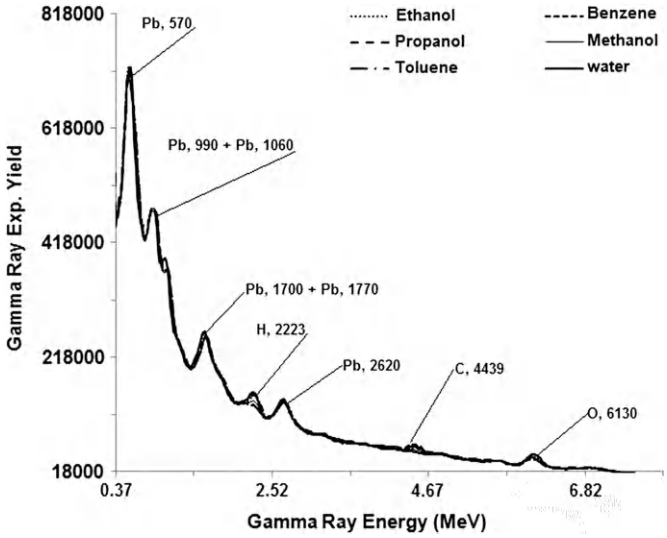

Fig. 6. Full prompt gamma ray spectra of 102×102 mm^2 (diameter $\times$ height) BGO gamma ray detector for benzene, ethanol, toluene, water and methanol samples.

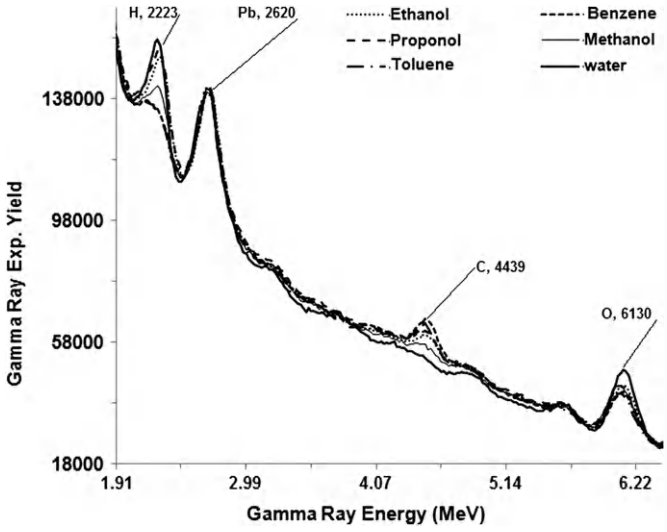

Fig. 7. Enlarged BGO detector prompt gamma ray spectra of benzene, propanol, water and methanol samples plotted over the 3.53–6.53 MeV energy range showing carbon and oxygen peaks along with associated escape peaks.

pulse height spectrum of the BGO detector due to the inelastic scattering of 14 MeV neutrons from the bulk samples and the shielding material over the 0.37–7.89 MeV energy range. Shown in Fig. 6 are the prompt gamma ray peaks from hydrogen, carbon and oxygen. Also shown in Fig. 6 are the gamma ray peaks due to the inelastic scattering of 14 MeV neutrons from lead shield and these are consistent with energies observed in the $LaBr_3$:Ce spectrum.

Fig. 7 is the enlarged portion of the pulse height spectrum of the BGO detector over the 1.91–6.22 MeV energy range showing increasing peak intensities of hydrogen and carbon peaks for samples with increasing concentrations of hydrogen and carbon listed in Table 1. Due to the large concentration of oxygen in the BGO detector, the oxygen peak intensity was insensitive to variation of oxygen concentration in the ethanol, methanol, benzene and water samples, but still it showed remarked increases in intensity of oxygen gamma rays for water sample containing oxygen contents comparable with detector oxygen contents. This is the main drawback of the BGO detector in detecting oxygen in bulk samples using the PGNAA technique.

4. Results and discussion

Data from the $LaBr_3$:Ce and the BGO detector for hydrogen, carbon and oxygen peaks in the respective pulse height spectra of the benzene, water, toluene, propanol, ethanol and methanol bulk samples were analyzed and the net counts under hydrogen, carbon and oxygen peaks were extracted by subtracting the container background spectra from the sample spectra. The net counts were then corrected for dead time and neutron flux variation. Finally, the gamma ray yield curves as a function of hydrogen, carbon and oxygen concentration in the bulk samples were generated. Net counts along with the background counts of carbon, oxygen and hydrogen peaks of the samples for the LaBr3:Ce and BGO detectors are listed in Table 2.

Figs. 8 and 9 show the gamma ray yield as a function of hydrogen, carbon and oxygen concentrations in benzene, water, propanol, ethanol and methanol samples measured with the $LaBr_3$:Ce detector. The lines in Figs. 8 and 9 represent results of hydrogen, carbon and oxygen prompt calculated gamma-ray yields from benzene, water, propanol, ethanol and methanol samples obtained through Monte Carlo calculation using MCNP4C code [4] following the procedure described elsewhere [15]. Figs. 10 and 11 show gamma ray yields as a function of hydrogen and carbon concentrations in benzene, water, ethanol and methanol samples measured with the BGO detector. The lines in Figs. 10 and 11 represent results of calculated yields of hydrogen and carbon prompt gamma-ray obtained from benzene, water, ethanol and methanol samples using Monte Carlo calculation.

The excellent agreement between the theoretical and experimental yields of hydrogen, carbon and oxygen prompt gamma-rays as a function of their respective concentrations recorded by the $LaBr_3$:Ce detector shows its suitability for hydrogen, carbon and oxygen measurements in contraband and explosive detection. However, for the BGO detector excellent agreement has been obtained between the theoretical and experimental yields for hydrogen and carbon only. Due to lack of sensitivity for oxygen measurement, the BGO detector is not suitable for oxygen determination.

Finally from the hydrogen, carbon and oxygen concentration measurements in benzene, water, propanol, ethanol and methanol bulk samples, the minimum detection limits (MDC) and its associated error σ_{MDC} were calculated for the KFUPM 14 MeV based PGNAA setup using the relation: $MDC = 4.653 \times (C/P) \times \sqrt{B}$ and $\sigma_{MDC} = (C/P) \times [\sqrt{(2B)}]$ for an elemental concentration C measured under a peak with net counts P and associated background counts B (under the peak) where the P and B counts integration is carried out for the same channel width and for the same amount of time. MDC equation is also called the Curie Equation of Minimum Detection Limit (MDL) of counts [13].

The minimum detection limits of KFUPM 14 MeV neutron based PGNAA setup for hydrogen, carbon and oxygen are listed in Table 3. These were found for $\emptyset 9 \times 14$ cm^2 cylindrical benzene, water, propanol, ethanol and methanol samples. The minimum detection limits of hydrogen and carbon using the BGO detector is lower than that of the $LaBr_3$:Ce detector because the BGO detector has a larger size.

5. Conclusion

Performance of $LaBr_3$:Ce and BGO gamma ray detectors were tested for detection of high energy prompt gamma rays from hydrogen, carbon and oxygen in ethanol, propanol, methanol, water and benzene samples using a 14 MeV neutron-based PGNAA setup. An excellent agreement has been observed between the experimental and theoretical yields of 2.22, 4.43 and 6.13 MeV

Table 2
Net and background counts from propanol, methanol, water, benzene, toluene and ethanol samples for $LaBr_3$:Ce and BGO detectors.

Sample	LaBr:Ce detector						BGO detector					
	Carbon		Oxygen		Hydrogen		Carbon		Oxygen		Hydrogen	
	Net counts	Background counts	Net counts	Background counts	Net counts	Background counts	Net counts	Background counts	Net counts	Background counts	Net counts	Background counts
Propanol	5392	56,050	1473	30,500	51,860	161,505	87,409	934,847	–	–	352,716	2,031,721
Water		–	4511	30,308	45,259	161,505	–	–	–	–	305,489	2,031,721
Benzene	8170	55,853	–	–	30,202	161,505	126,939	934,847	–	–	228,345	2,031,721
Methanol	3353	55,325	2339	29,808	46,514	161,505	68,054	934,847	–	–	177,114	2,031,721
Toluene	–	–	–	–	–	–	122,071	934,847	–	–	244,188	2,031,721
Ethanol	–	–	–	–	–	–	55,372	934,847	–	–	–	–

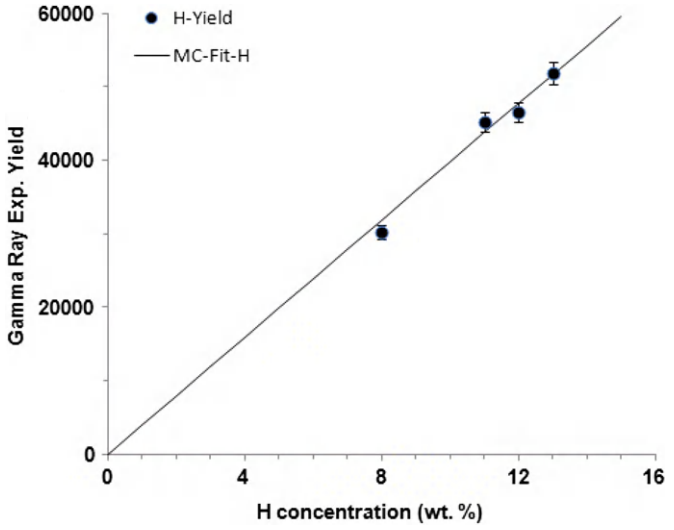

Fig. 8. Integrated normalized experimental yield of hydrogen prompt gamma rays taken with the $LaBr_3$:Ce detector, plotted as a function of hydrogen concentration in benzene, propanol, water and methanol samples. The solid line is a Monte Carlo fit to the experimental data.

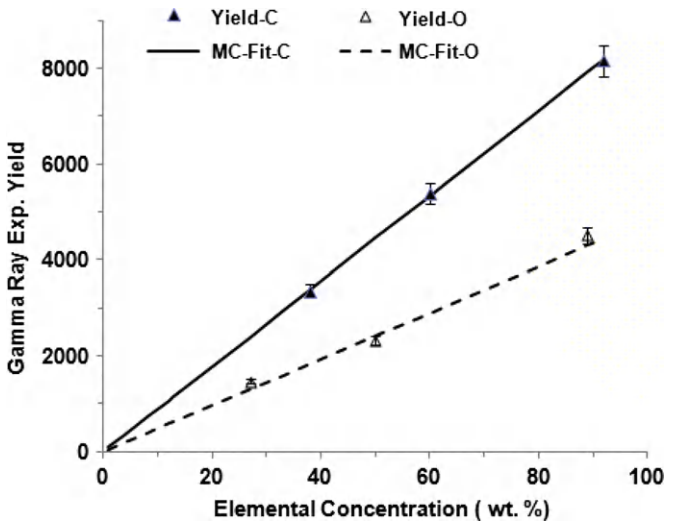

Fig. 9. Integrated normalized experimental yield of carbon and oxygen prompt gamma rays taken with the $LaBr_3$:Ce detector, plotted as a function of carbon and oxygen concentrations in benzene, propanol, water and methanol samples. The solid line is a Monte Carlo fit to the experimental data.

gamma rays as a function of hydrogen, carbon and oxygen concentrations in ethanol, propanol, methanol, water and benzene samples. The tests show that, inspite of its intrinsic activity, the

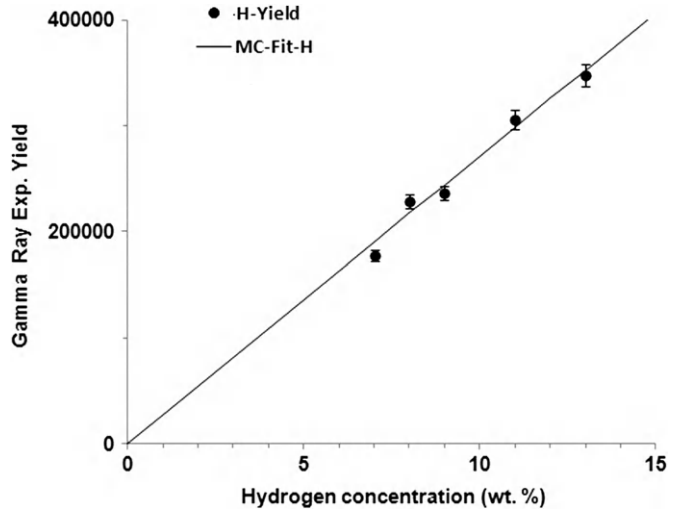

Fig. 10. Integrated normalized experimental yield of hydrogen prompt gamma rays taken with the BGO detector, plotted as a function of hydrogen concentration in benzene, propanol, toluene, water and methanol samples. The solid line is a Monte Carlo fit to the experimental data.

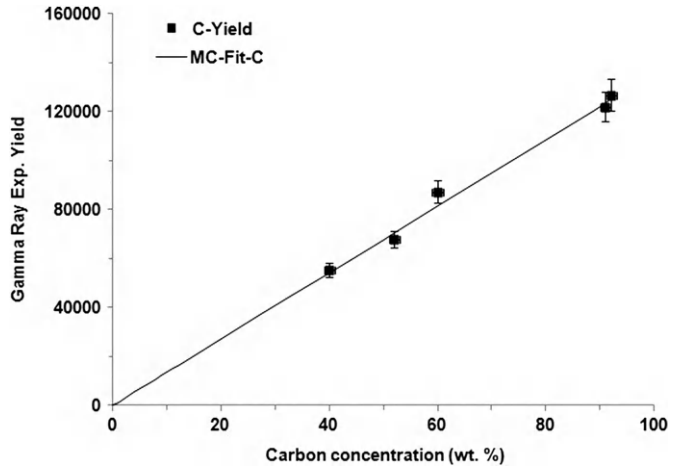

Fig. 11. Integrated normalized experimental yield of carbon prompt gamma rays taken with the BGO detector, plotted as a function of carbon concentration in benzene, propanol, toluene, water and methanol samples. The solid line is a Monte Carlo fit to the experimental data.

$LaBr_3$:Ce gamma ray detector has superior performance than the BGO detector for the detection of hydrogen, carbon and oxygen in ethanol, propanol, ethanol, methanol, water and benzene bulk samples. Due to its large oxygen content, the BGO detector is not suitable for the detection of oxygen.

Table 3
MDC of hydrogen, carbon and oxygen for KFUPM 14 MeV neutron-based PGNAA setup using $LaBr_3$:Ce and BGO detectors.

Detector type	MDCH (wt%)	MDCC (wt%)	MDCO (wt%)
$LaBr_3$:Ce	0.5 ± 0.1	12.2 ± 3.8	15.8 ± 4.8
BGO	0.3 ± 0.1	3.2 ± 1.0	–

Acknowledgment

This study is part of project #IN090033 funded by the King Fahd University of Petroleum and Minerals, Dhahran, Saudi Arabia. The support provided by the Department of Physics and Department of Chemistry, King Fahd University of Petroleum and Minerals, Dhahran, Saudi Arabia, is also acknowledged.

References

[1] A.A. Aksoy, F.Z. Naqvi, M. Khiari, A. Raashid, R.E. Coban, Abdel-Aal, H. Al-Juwair, Nuclear Instruments and Methods in Physics Research, Section A: Accelerators, Spectrometer, Detectors and Associated Equipment 332 (1993) 506.
[2] D. Alexiev, L. Mo, D.A. Prokopovich, M.L. Smith, M. Matuchova, IEEE Transactions on Nuclear Sciences NS55 (3) (2008) 1174.
[3] M. Balcerzyk, M. Moszyński, M. Kapusta, Nuclear Instruments and Methods in Physics Research, Section A: Accelerators, Spectrometers, Detectors and Associated Equipment 537 (2005) 50.
[4] J.F. Briesmeister (Ed.), MCNP4C—A General Monte Carlo N-Particles Transport Code, Los Alamos National Laboratory Report, LA-12625-M, Version 4C, 1997.
[5] A. Buffler, Radiation Physics and Chemistry 71 (2004) 853.
[6] M. Ciema, D. Balabanski, M. Csatlo, J.M. Daugas, G. Georgiev, J. Gulya, M. Kmiecik, A. Krasznahorkay, S. Lalkovski, A. Lefebvre-Schuhl, R. Lozeva, A. Maj, A. Vitez, Nuclear Instruments and Methods in Physics Research 608 (2009) 76.
[7] S. Davorin, S. Pesente, G. Nebbia, G. Viesti, V. Valkovic, Nuclear Instruments and Methods in Physics Research B 261 (2007) 321.
[8] C. Eleon, B. Perot, C. Carasco, D. Sudac, J. Obhodas, V. Valkovic, Nuclear Instruments and Methods in Physics Research A 629 (2011) 220.
[9] F.C. Engesser, W.E. Thompson, Journal of Nuclear Energy 21 (1967) 487.
[10] A. Favalli, H.C. Mehner, V. Ciriello, B. Pedersen, Applied Radiation and Isotopes 68 (2010) 901.
[11] F.J.O. Ferreira, V.R. Crispim, A.X. Silva, Applied Radiation and Isotopes 68 (2010) 1012.
[12] A. Iltis, M.R. Mayhugh, P. Menge, C.M. Rozsa, O. Selles, V. Solovyev, Nuclear Instruments and Methods in Physics Research, Section A: Accelerators, Spectrometers, Detectors and Associated Equipment 563 (2006) 359.
[13] G.F. Knoll, Radiation Detection and Measurements, John Willey Publisher, 2000.
[14] P.R. Menge, G. Gautier, A. Iltis, C. Rozsa, V. Solovyev, Nuclear Instruments and Methods in Physics Research, Section A: Accelerators, Spectrometers, Detectors and Associated Equipment 579 (2007) 6.
[15] A.A. Naqvi, Zameer Kalakada, M.S. Al-Anezi, M. Raashid, Khateeb-ur Rehman, M. Maslehuddin, M.A. Garwan, F.Z. Khiari, A.A. Isab, O.S.B. Al-Amoudi, Nuclear Instruments and Methods in Physics Research A 665 (2011) 74.
[16] A. Owens, A.J.J. Bos, S. Brandenburg, C. Dathy, P. Dorenbos, S. Kraft, R.W. Ostendorf, V. Ouspenski, F. Quarati, Nuclear Instruments and Methods in Physics Research, Section A: Accelerators, Spectrometers, Detectors and Associated Equipment 574 (2007) 110.
[17] E.H. Seabury, B.W. Blackburn, D.L. Chichester, C.J. Wharton, A.J. Caffrey, Nuclear Instruments and Methods in Physics Research B 261 (2007) 839.
[18] E.H. Seabury, A.J. Caffery, Explosive Detection and Identification by PGNAA, Report #INL/EXT-06-01210 Idaho National Laboratory, Idaho Falls, Idaho 83415, USA, April 2006.
[19] K.S. Shah, J. Glodo, M. Klugerman, L. Cirignano, W.W. Moses, S.E. Derenzo, M.J. Weber, Nuclear Instruments and Methods in Physics Research, Section A: Accelerators, Spectrometers, Detectors and Associated Equipment 505 (2003) 76.
[20] T.J. Shaw, D. Brown, J. D'Arcy, et al., Applied Radiation and Isotopes 63 (2005) 779.